Journal of the European Ceramic Society 23 (2003) 1123–1130

www.elsevier.com/locate/jeurceramsoc

High strength B_4C–TiB_2 composites fabricated by reaction hot-pressing

Suzuya Yamada[a,*], Kiyoshi Hirao[b], Yukihiko Yamauchi[b], Shuzo Kanzaki[b]

[a]*Synergy Ceramics Laboratory, Fine Ceramics Research Association, Nagoya, Aichi 463-8687, Japan*

[b]*Synergy Materials Research Center, National Institute of Advanced Industrial Science and Technology Nagoya, Aichi 463-8687, Japan*

Received 8 February 2002; received in revised form 16 July 2002; accepted 27 July 2002

Abstract

B_4C based composites with 20 mol% TiB_2 were fabricated by reaction hot-pressing of four different submicron size B_4C powders with the addition of nanometer size TiO_2 and C powders at 2000 °C, and their mechanical properties were examined. A B_4C–TiB_2 composite with both high strength of 866 MPa and modest fracture toughness of 3.2 MPa $m^{1/2}$ could be obtained using B_4C powder with a mean particle size of 0.50 μm and total metal impurity 0.3–0.5 wt.% (Al + Fe). It seems that this extremely high strength is attributed to the fine-grained B_4C microstructure, uniform dispersion of TiB_2 particles and improvement of fracture toughness.
© 2002 Elsevier Science Ltd. All rights reserved.

Keywords: B_4C; Borides; Composites; Strength; Toughness; Toughening; TiB_2

1. Introduction

Boron carbide (B_4C) possesses unique physical and thermal properties such as high elastic modulus, high melting point, good chemical stability and high neutron absorption cross-section. In addition, B_4C ceramics exhibit excellent mechanical properties such as high hardness and high wear resistance.[1–5] They are currently used in nuclear energy and high-temperature thermoelectric conversion. However, their widespread application has been restricted mainly due to their low strength and fracture toughness as well as poor sinterability due to a low self-diffusion coefficient. Several additives have been investigated in order to promote the sinterability of B_4C. The addition of carbon has been found to be effective in improving the densification of B_4C,[6–10] and a B_4C ceramic with a relative density of 96.4% has been fabricated by pressureless sintering at 2150 °C with the addition of carbon.[10] Full densification of this material could be achieved by means of a post-HIP treatment. Its flexural strength was increased from 475 to 579 MPa by this treatment, although the fracture toughness decreased from 2.8 to 2.4 MPa $m^{1/2}$. Aluminium and Al containing compounds such as AlF_3 have also been used for densification of B_4C. A high relative density of 95% was achieved with the addition of 1 mass% Al by pressureless sintering at 2200 °C.[11] The addition of a small amount of Al_2O_3 greatly improved the sinterability of B_4C, and a ceramic with flexural strength of 550 MPa was obtained by hot-pressing B_4C powder with 2.5 vol.% Al_2O_3 at 2000 °C.[12] The effect of other additives such as SiC, TiC, WC and BN have also been investigated, with limited success.[13–16]

The purpose of previous investigations was mainly to enhance the densification and, thereby, to increase the strength of B_4C ceramics. On the other hand, B_4C ceramics with dispersed TiB_2 particles have been investigated in order to improve both strength and toughness.[17–20] The improvement of fracture toughness achieved by TiB_2 additions has been explained in terms of microcrack formation caused by the thermal expansion mismatch between dispersed particles and the matrix.[18–21] Skorokhod and Krstic have successfully fabricated a B_4C–TiB_2 composite with a flexural strength of 621 MPa and a fracture toughness of 6.1 MPa $m^{1/2}$ by reaction hot-pressing of submicron size B_4C with the addition of submicron size TiO_2 and C at

* Corresponding author at present address: Research Center, Denki Kagaku Kogyo K. K. Machida-city, Tokyo 194-8560, Japan. Tel. +1-81-42-721-3642; fax: +1-81-42-721-3693.

E-mail address: suzuya-yamada@denka.co.jp (S. Yamada).

0955-2219/03/$ - see front matter © 2002 Elsevier Science Ltd. All rights reserved.
PII: S0955-2219(02)00274-1

2000 °C.[20] The high strength of this material was attributed to the combination of high fracture toughness and fine microstructure.

Mechanical properties of two phase composites are influenced remarkably by their microstructure.[24] It is considered that the microstructure of B_4C ceramics is strongly affected by the characteristics of the B_4C starting powder, such as mean particle size and impurities which promote densification. However, there have been a very limited number of such studies concerning B_4C–TiB_2 composites. In the present study, the effect of characteristics of B_4C powders on microstructure and mechanical properties of B_4C–TiB_2 ceramics fabricated by reaction hot-pressing powder mixtures of B_4C, TiO_2 and C has been investigated using commercially available B_4C powders with different particle sizes and impurities. In order to prepare B_4C ceramics with uniformly dispersed TiB_2 particles, nanometer size TiO_2 powder and carbon black were used as starting materials. The microstructure and mechanical properties such as flexural strength and fracture toughness of specimens were examined and compared with monolithic B_4C.

2. Experimental procedure

Four kinds of B_4C powders were used as raw materials: these are referred to as powder A (Grade HS, H. C. Starck GmbH, Berlin, Germany), powder B (Grade #1200, Denki Kagaku Kogyo Co., Tokyo, Japan), powder C (Grade 3000F, Elektroschmelzwerk Kempten GmbH, Munchen, Germany) and powder D (Grade #1500, Denki Kagaku Kogyo Co., Tokyo, Japan). The mean particle size of the powders, measured by a particle size analyzer (UPA 150, Microtrac Inc., Montgomeryville, USA), are shown in Table 1. All of the B_4C powders had a mean particle size of about 0.5 μm. However, it should be noticed that, in powder A, there existed a small amount of large particles as shown in Fig. 1. Carbon black (Grade Regal 330R, Cabot Co., Boston, USA) was used as the carbon source, and had a specific surface area of 88.1 m^2/g. The nanometer size TiO_2 powder (Grade Nano Tek, C.I Kasei Co., Tokyo, Japan) used in this study was produced by the vapour phase reaction method, and consisted of spherical particles with a mean particle size of 28 nm calculated from a specific surface area of 54.6 m^2/g.

Each of the four B_4C powders was mixed with 14.5 mol% TiO_2 and 21.5 mol% C using a planetary ball mill with a SiC pot and SiC balls in methanol for 1 h. This starting composition was determined so as to form B_4C–20 mol% TiB_2 composition according to Eq. (1).

$$B_4C + 2\ TiO_2 + 3C = 2\ TiB_2 + 4CO \quad (1)$$

The slurry was dried in a rotary vacuum evaporator for 1 h, followed by drying at 115 °C for 24 h. The powder mixture was passed through a 60 mesh sieve. Reaction hot-pressing was performed using a carbon resistance furnace in a rectangular graphite die (47 mm×42 mm) at 2000 °C for 1 h with an applied load of 50 MPa under 0.1 MPa argon pressure. The temperature was monitored by an optical pyrometer, which was calibrated in advance using a thermocouple. The heating rates were 40 °C/min from room temperature to 1200 °C, 20 °C/min to 1500 °C and 10 °C/min to 2000 °C. For the sake of comparison, monolithic B_4C specimens without TiB_2 were also fabricated by the same procedure.

For measuring mechanical properties, test pieces were cut from the hot-pressed specimens and ground with a 400-grit diamond wheel to dimensions of 42 mm×4 mm×3 mm. The flexural strength was measured by a four-point bending test with inner and outer spans of 10 and 30 mm, respectively. The fracture toughness, K_{IC}, was measured by the SEPB method.[23] The densities of the specimens were determined by the water displacement method. Phase identification was performed by X-ray diffractometry (XRD: RINT 2500, Rigaku, Tokyo, Japan) with CuK_α radiation. In order to observe the microstructure, specimens were polished with diamond slurry down to 1 μm. Some specimens were etched with Murakami's reagent [10 g of NaOH and 10 g of $K_3Fe(CN)_6$ in 100 ml H_2O at 110 °C]. Microstructural analysis was carried out using scanning electron microscopy (SEM: JSM5600, Jeol, Tokyo, Japan). The grain size of B_4C and the mean particle size of TiB_2 were measured by means of an image analysis (Scion Image, Scion Co., MD, USA).

Table 1
Characteristics of B_4C starting powders

		Powder A	Powder B	Powder C	Powder D
Mean particle size	(μm)	0.54	0.50	0.43	0.40
Specific surface area	(m^2/g)	17.6	21.0	15.3	22.4
Oxygen	(%)	1.7	2.5	2.0	3.6
Metal impurities	Fe (ppm)	260	2000	140	4000
	Al (ppm)	80	1200	50	1100

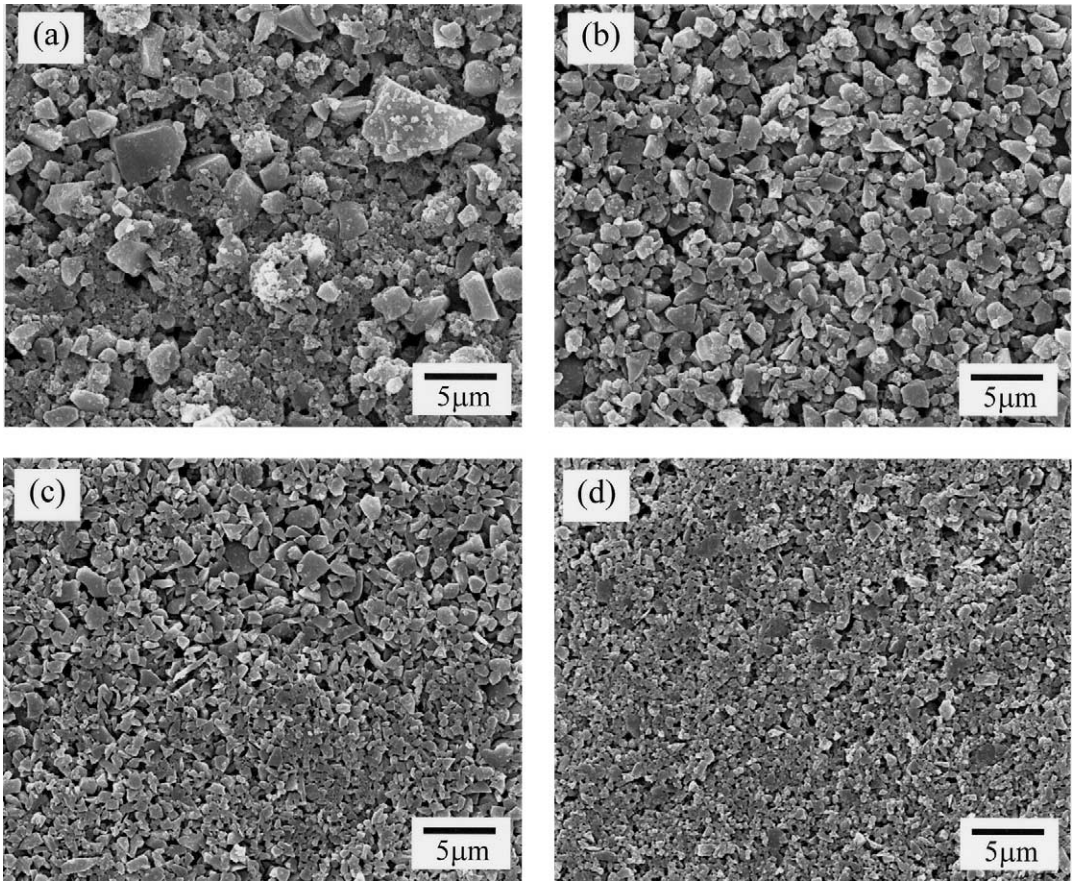

Fig. 1. SEM photographs of B_4C starting powders: (a) powder A, (b) powder B, (c) powder C and (d) powder D.

3. Results and discussion

In the case of monolithic B_4C ceramics, full densification could be achieved in the B and D specimens, whilst relative densities of the specimens from the A and C samples were slightly lower at 98.1 and 99.7% of theoretical density, respectively (Table 2). It has been reported that the addition of 1 vol.% Al_2O_3 (correspondingly to 0.83 mass% Al) greatly improved the densification of B_4C ceramic,[12] and that the densification of B_4C–TiB_2 composite was enhanced by the addition of 1 wt.% Fe.[17] It seems, therefore, that the high levels of aluminium and iron impurities in the B and D powders contributed to full densification of the specimens. On the contrary, a low impurity level as well as a relatively large particle size in the A powder resulted in the low density of the specimen. Fig. 2 shows polished and chemically etched surfaces of the monolithic B_4C specimens fabricated by hot-pressing the four kinds of B_4C powders at 2000 °C. In the specimens prepared from the A and C powders, the grain size of the hot-pressed specimens was almost the same as the particle

Table 2
Densities and mechanical properties of monolithic B_4C and B_4C–TiB_2 specimens

Sample	B_4C powder	Specimen	Theoretical density (g/cm^3)	Relative density (%)	Flexural strength (MPa)	Fracture toughness (MPa m$^{1/2}$)	TiB_2 particle size (μm)
Sample A	Powder A	Monolithic B_4C	2.52	98.1	479	2.60	–
Sample A-T		B_4C–20 mol% TiB_2	2.82	~100	659	2.49	1.07
Sample B	Powder B	Monolithic B_4C	2.52	~100	582	2.40	–
Sample B-T		B_4C–20 mol% TiB_2	2.82	~100	866	3.20	2.20
Sample C	Powder C	Monolithic B_4C	2.52	99.7	615	2.61	–
Sample C-T		B_4C–20 mol% TiB_2	2.82	~100	718	2.76	0.76
Sample D	Powder D	Monolithic B_4C	2.52	~100	480	2.47	–
Sample D-T		B_4C–20 mol% TiB_2	2.82	~100	808	3.02	1.75

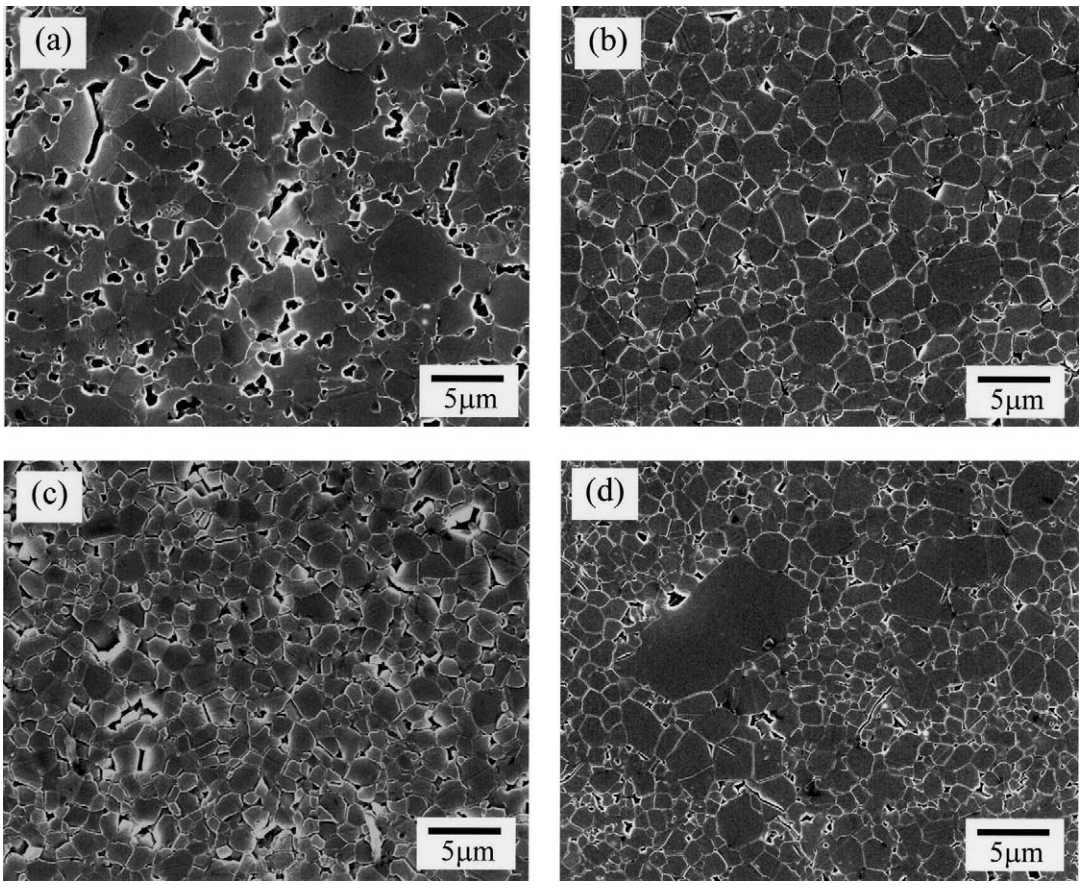

Fig. 2. Microstructures of monolithic B_4C specimens fabricated using four kinds of B_4C powders: (a) powder A, (b) powder B, (c) powder C and (d) powder D.

size of the starting powders (Fig. 1). On the other hand, substantial grain growth was observed for the specimens from powders B and D. For the sample from powder D, in particular, abnormal grain growth took place. It is thought that aluminium and iron impurities enhance not only densification but also grain growth.

All of the B_4C–20 mol% (15 vol.%) TiB_2 specimens fabricated by reaction hot-pressing exhibited full densities (Table 2). Compared with the monolithic B_4C specimens, densification of the B_4C–TiB_2 composite specimens from the A and C powders was enhanced by reaction hot-pressing. Typical X-ray diffraction patterns of the starting mixtures and hot-pressed specimens are shown in Fig. 3. For the starting powder mixture, B_4C and two types of crystalline TiO_2 phases were identified plus an additional small peak at 35.7° which corresponds to diffraction from SiC (102). The SiC contamination is thought to originate from the SiC pot and balls used during mixing. The carbon phase was not observed owing to the low crystallinity of carbon black. XRD analysis of the B_4C–TiB_2 specimen revealed that it was a composite of B_4C and TiB_2 phases with a trace of SiC. No other phase was identified.

Fig. 4 shows microstructures observed in the polished surfaces of the B_4C–TiB_2 specimens. In the photographs, TiB_2 particles appear as white spots due to the larger atomic weight of Ti compared to B and C. In all of the specimens, TiB_2 particles were dispersed in the B_4C matrix, but their morphology was quite different depending on the type of B_4C powder used as starting material. In the case of the B_4C–TiB_2 specimens from the both the A and C powders (Fig. 4a, c), the mean size of TiB_2 particles was small at 1.07 and 0.76 μm, respec-

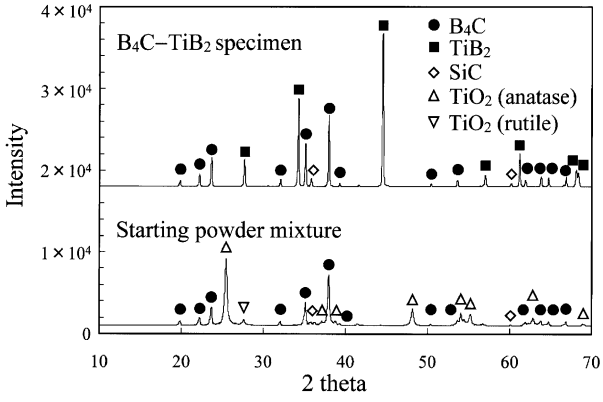

Fig. 3. X-ray diffraction patterns of starting powder mixture and B_4C–TiB_2 specimen fabricated using powder B.

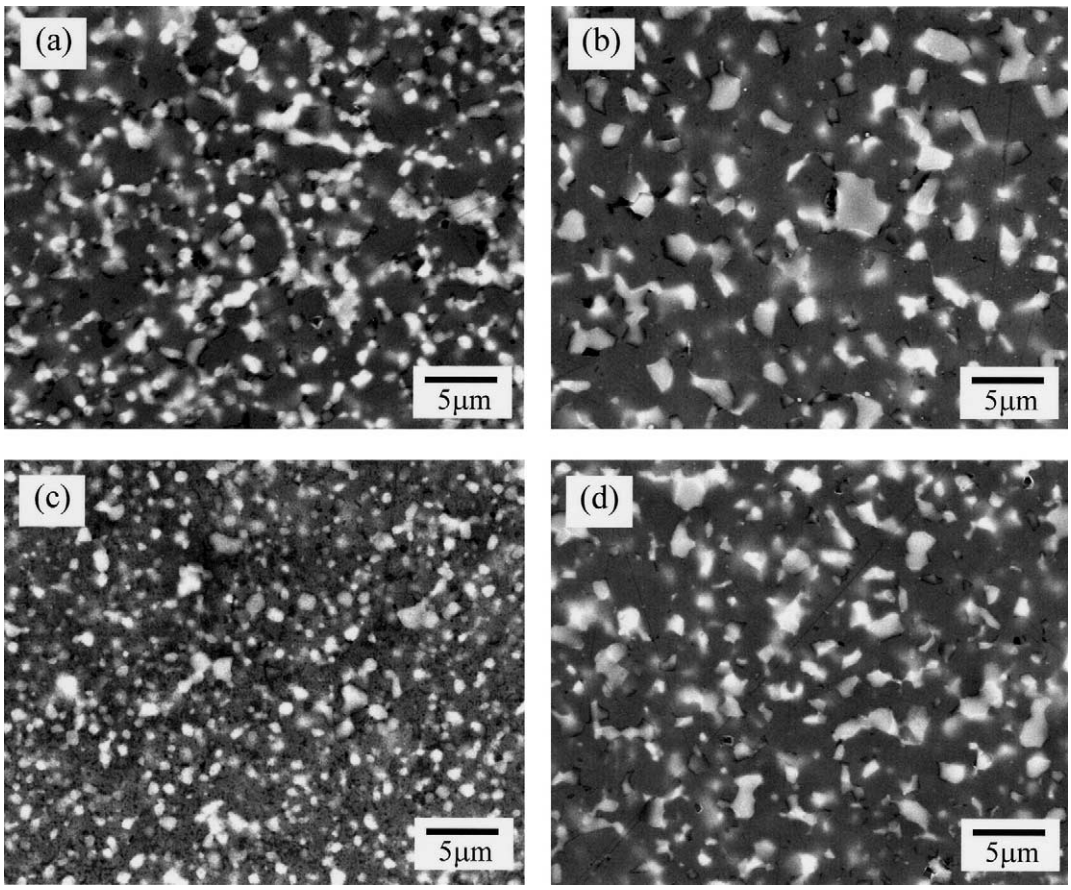

Fig. 4. Microstructures of B_4C–TiB_2 specimens fabricated using four kinds of B_4C powders: (a) powder A, (b) powder B, (c) powder C and (d) powder D.

tively (Table 2). A large number of aggregated TiB_2 particles existed in the specimen from powder A, whereas the particles were highly dispersed in the specimen from powder C. On the contrary, relatively large TiB_2 particles with mean sizes of 2.20 and 1.75 μm in diameter were dispersed in the B_4C–TiB_2 specimens from powders B and D (Fig. 4b,d). The size of TiB_2 particles was uniform for the specimen from powder B, whereas, for the specimen fabricated using powder D, there were a number of smaller sized TiB_2 particles. Skorokhod et al. stated that the growth of TiB_2 particles in a B_4C–TiB_2 composite occurs mainly through the diffusion along the B_4C grain boundaries.[22] It was thought that the diffusion transport of TiB_2 was promoted by the presence of the aluminium and iron impurities in the specimens from powders B and D. Fig. 5 shows the grain size distributions of B_4C for the monolithic and B_4C–TiB_2 composite specimens fabricated using the powder D. Larger B_4C grains with grain size over 3 μm were present in the monolithic B_4C specimen, whereas these large grains were not present in the B_4C–TiB_2 specimen. It was thought that the abnormal grain growth of B_4C was inhibited by TiB_2 particle dispersion for the B_4C-TiB_2 specimen.[24]

Fig. 6 shows the flexural strength and the fracture toughness of the B_4C specimens with and without TiB_2 fabricated using the four kinds of B_4C powders. The fracture toughness of the monolithic specimens were as low as 2.4–2.6 MPa $m^{1/2}$. As compared with monolithic specimens, the fracture toughness of the composite specimens from the powders B, C and D were increased by the dispersed TiB_2 particles. However, that of the composite specimen from the powder A showed no improvement over the monolithic material.

The thermal expansion coefficient of TiB_2 is larger than that of the B_4C matrix,[1] such that residual stress is generated around the TiB_2 particles during cooling. This residual stress results in the formation of microcracks and, to some degree, deflection of propagating cracks, which leads to improvement in fracture toughness of composite materials.[18–21] In order to examine the crack propagating behaviour for the B_4C–TiB_2 specimens, an indentation on the polished surface was carried out using a Vickers diamond indenter. As shown in Fig. 7, crack deflection occurred around the TiB_2 particles for the B_4C–TiB_2 specimen from the powder B.

Over a critical particle size, however, the fracture toughness decreases with increasing the dispersed parti-

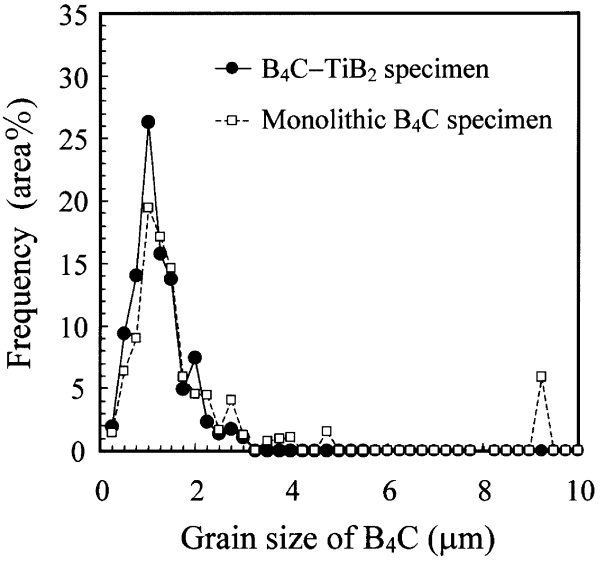

Fig. 5. Distributions of grain size of B_4C for monolithic B_4C and B_4C–TiB_2 specimens fabricated using powder D.

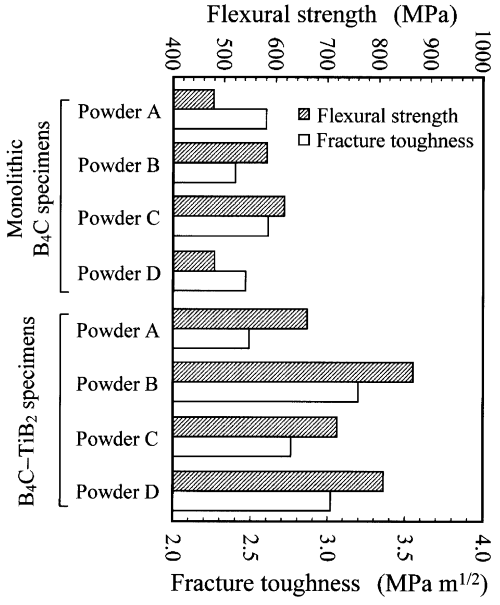

Fig. 6. Mechanical properties of monolithic B_4C and B_4C–TiB_2 specimens.

cle size since cracks develop spontaneously during cooling. As shown in Fig. 8, there is a clear tendency for the fracture toughness to increase with an increase in the size of TiB_2 particle among the B_4C–TiB_2 specimens from powders B, C and D. However, fracture toughness was not improved in the specimen from powder A. It seems that aggregation of TiB_2 particles forms a three dimensional network structure in this composite specimen (Fig. 4a), which results in the lower residual stress.

As shown in Fig. 6, the flexural strength for the monolithic specimen from powder A exhibited a low strength of 479 MPa, owing to the low density. In addition, the large B_4C particles formed by the abnormal grain growth acted as the fracture origin for the specimen from powder D (Fig. 2d), consequently, a low flexural strength of 480 MPa was obtained. Relatively high flexural strength of 615 MPa was obtained for the specimen from powder C. It seems that it is attributed to the fine grained microstructure shown in Fig. 2c. Flexural strength of 582 MPa was obtained for the specimen from powder B. The flexural strength for all the specimens were improved by reaction hot-pressing (Fig. 6).

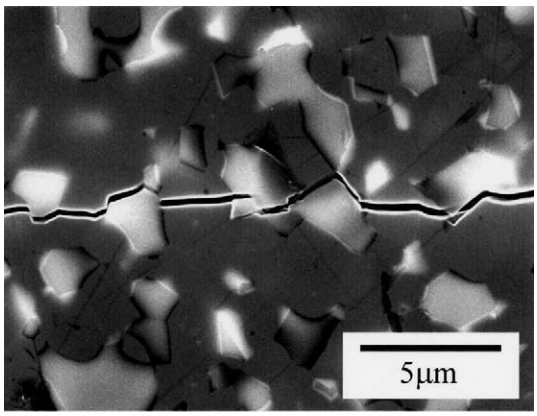

Fig. 7. Crack deflection on B_4C–TiB_2 specimen fabricated using powder B.

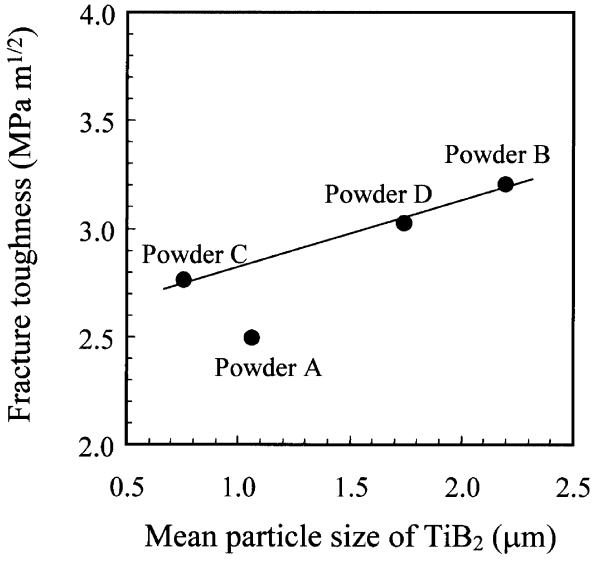

Fig. 8. Fracture toughness of B_4C–TiB_2 specimens as a function of mean particle size of TiB_2.

Fig. 9 shows the relationship between the flexural strength and fracture toughness for all of the specimens. The flexural strength was clearly proportional to the fracture toughness for the composite specimens, although plots for the monolithic specimens were randomly scattered. The critical flaw sizes of these specimens are calculated based on Griffith's equation ($c = 2K_{IC}^2/\pi\sigma_f^2$) using the experimental values of the flexural strength (σ_f) and the fracture toughness (K_{IC}).[19]

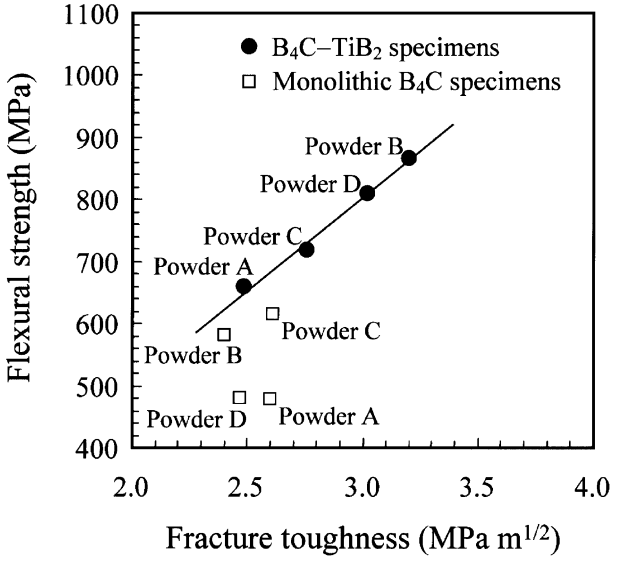

Fig. 9. Flexural strength of monolithic B_4C and B_4C–TiB_2 specimens as a function of fracture toughness.

The critical flaw sizes for all of the B_4C–TiB_2 specimens were of the same order of 8.7–9.4 μm, whereas those of the monolithic B_4C specimens were larger compared to the B_4C–TiB_2 specimens and varied from 10.8 to 18.8 μm. These large critical flaw sizes of the monolithic specimens can be contributed to the low density and the abnormal B_4C grain growth. Full densification was achieved for all the B_4C–TiB_2 specimens, and the abnormal grain growth was inhibited by the dispersion of TiB_2 particles. Therefore, the critical flaw sizes of the composite specimens became smaller and more uniform. High flexural strength over 800 MPa was obtained for the B_4C–TiB_2 specimens from powders B and D. In particular, both extremely high strength of 866 MPa and modest fracture toughness of 3.2 MPa $m^{1/2}$ could be achieved in the B_4C–TiB_2 specimen from powder B.

4. Conclusions

B_4C–20 mol% TiB_2 ceramic composites were fabricated by reaction hot-pressing powder mixtures of four different submicron size B_4C, nanometer size TiO_2 and carbon black at 2000 °C. B_4C–TiB_2 specimens exhibited a composite microstructure where TiB_2 particles were dispersed uniformly in a fine grained B_4C matrix. The abnormal grain growth of B_4C was inhibited, and the fracture toughness was increased for some of the B_4C–TiB_2 specimens. It appears that this improvement in toughness is due to the formation of microcracks and deflection of propagating cracks caused by the thermal expansion mismatch between TiB_2 particles and B_4C matrix. By using B_4C starting powders with higher aluminium and iron impurities content, the growth of TiB_2 particles was promoted and, therefore, fracture toughness increased further. Both high strength of 866 MPa and modest fracture toughness of 3.2 MPa $m^{1/2}$ could be achieved in the B_4C–TiB_2 specimen fabricated using B_4C powder with a mean particle size of 0.50 μm and total metal impurity between 0.3 and 0.5 wt.% (aluminium plus iron).

Acknowledgements

This work has been supported by METI, Japan, as part of the Synergy Ceramics Project. Part of the work has been supported by NEDO. The authors are members of the Joint Research Consortium of Synergy Ceramics. The authors are grateful to Dr. Shuji Sakaguchi (AIST) for valuable comments.

References

1. Nishikawa, H., Powder or boron compound at present. *Ceramics*, 1987, **22**, 40–45.
2. Takagi, K., Boride materials. *Metals and Technologies*, 1993, **1**, 23–28.
3. Nishiyama, K., Sintering and tribology of boride hard materials. *J. Jpn. Soc. Powder Powder Met.*, 1996, **43**, 464–471.
4. Johnson, W. C., Advanced materials and powders. *Am. Ceram. Soc. Bull.*, 2001, **80**, 64–66.
5. Larsson, P., Axen, N. and Hogmark, S., Improvements of the microstructure and erosion resistance of boron carbide with additives. *J. Mater. Sci.*, 2000, **35**, 3433–3440.
6. Thevenot, F., Boron carbide—a comprehensive review. *J. Eur. Ceram. Soc.*, 1990, **6**, 205–225.
7. Thevenot, F., A review on boron carbide. *Key Eng. Mater.*, 1991, **56–57**, 59–88.
8. Suzuki, H., Hase, T. and Maruyama, T., Effect of carbon on sintering of boron carbide. *Yogyo-Kyokai-Shi*, 1979, **87**, 430–433.
9. Schwetz, K. A. and Grellner, W., The influence of carbon on the microstructure and mechanical properties of sintered boron carbide. *J. Less-Common Met.*, 1981, **82**, 37–47.
10. Schwetz, K. A., Sigl, L. S. and Pfau, L., Mechanical properties of injection molded B_4C-C ceramics. *J. Solid State Chem.*, 1997, **133**, 68–76.
11. Kanno, Y., Kawase, K. and Nakano, K., Additive effect on sintering of boron carbide. *Yogyo-Kyokai-Shi*, 1987, **95**, 1137–1140.
12. Kim, H. W., Koh, Y. H. and Kim, H. E., Densification and mechanical properties of B_4C with Al_2O_3 as a sintering aid. *J. Am. Ceram. Soc.*, 2000, **83**, 2863–2865.
13. Thevenot, F., Sintering of boron carbide and boron carbide-silicon carbide two-phase materials and their properties. *J. Nucl. Mater.*, 1988, **152**, 154–162.
14. Sigl, L. S., Processing and mechanical properties of boron carbide sintered with TiC. *J. Eur. Ceram. Soc.*, 1998, **18**, 1521–1529.
15. Zakhariev, Z. and Radev, D., Properties of polycrystalline boron carbide sintered in the presence of W_2B_5 without pressing. *J. Mater. Sci. Lett.*, 1988, **7**, 695–696.
16. Ruh, R., Kearns, M., Zangvil, A. and Xu, Y., Phase and property studies of boron carbide-boron nitride composites. *J. Am. Ceram. Soc.*, 1992, **75**, 864–872.
17. Kim, D. K. and Kim, C. H., Pressureless sintering and micro-

structural development of B_4C-TiB_2 based composites. *Adv. Ceram. Mater*., 1988, **3**, 52–55.
18. Tuffe, S., Dubois, J., Fantozzi, G. and Barbier, G., Densification, microstructure and mechanical properties of TiB_2-B_4C based composites. *Int. J. Refr. Metals Hard Mater*., 1996, **14**, 305–310.
19. Skorokhod, V., Vlajic, M. D. and Krstic, V. D., Mechanical properties of pressureless sintered boron carbide containing TiB_2 phase. *J. Mater. Sci. Lett*., 1996, **15**, 1337–1339.
20. Skorokhod, V. and Krstic, V. D., High strength-high toughness B_4C-TiB_2 composites. *J. Mater. Sci. Lett*., 2000, **19**, 237–239.
21. Sigl, L. S. and Kleebe, H. J., Microcracking in B_4C-TiB_2 composites. *J. Am. Ceram. Soc*., 1995, **78**, 2374–2380.
22. Skorokhod, V. V., Vlajic, M. D. and Krstic, V. D., Pressureless sintering of B_4C-TiB_2 ceramic composites. *Materials Science Forum*, 1998, **282–283**, 219–224.
23. Nose, T. and Fujii, T., Evaluation of fracture toughness for ceramic materials by a single-edge-precracked-beam method. *J. Am. Ceram. Soc*., 1988, **71**, 328–333.
24. Yasuoka, M., Brito, M. E., Hirao, K. and Kanzaki, S., Effect of dispersed particle size on mechanical properties of alumina/ non-oxides composites. *J. Ceram. Soc. Jpn*., 1993, **101**, 889–894.